Carbohydrate Polymers 180 (2018) 314–327

Contents lists available at ScienceDirect

Carbohydrate Polymers

journal homepage: www.elsevier.com/locate/carbpol

Research Paper

Purification and Characterisation of κ-Carrageenan Oligosaccharides Prepared by κ-Carrageenase from *Thalassospira* sp. Fjfst-332

Juanjuan Guo[a,b,c], Zhichang Zheng[a,b,c], Xu Lu[a,b,c], Shaoxiao Zeng[a,b,c], Chi Chen[d], Longtao Zhang[a,b,c], Baodong Zheng[a,b,c,*]

[a] College of Food Science, Fujian Agriculture and Forestry University, Fuzhou, Fujian 350002, China
[b] China-Ireland International Cooperation Centre for Food Material Science and Structure Design, Fujian Agriculture and Forestry University, Fuzhou, Fujian 350002, China
[c] Fujian Provincial Key Laboratory of Quality Science and Processing Technology in Special Starch, Fujian Agriculture and Forestry University, Fuzhou, Fujian 350002, China
[d] Department of Food Science and Nutrition, University of Minnesota,St. Paul, MN, USA

ARTICLE INFO

Keywords:
κ-Carrageenan oligosaccharides
MPLC-ELSD
Anti-inflammatory
ROS
Structure-function relationship

ABSTRACT

κ-Carrageenan oligosaccharides (KCOs) are promising agents for treating inflammatory diseases. However, the lack of purification and structural elucidation of KCOs has limited structure-function evaluation. In this study, using a system coupling medium pressure liquid chromatography (MPLC) with an evaporative light scattering detector (ELSD), four types of KCOs were separated. The total yield of the four KCO powders was ~5.02% after purification (KCOs/κ-carrageenan, w/w). Their structural identities were characterised by ESI-MS, CID-MS/MS and NMR, as κ-neocarrabiose (α-DA-1,3-G4Srα/β), κ-neocarratetraose (α-DA-1,3-β-G4S-1,4-α-DA-1,3-G4Srα/β), κ-neocarrahexaose (α-DA-1,3-β-G4S-1,4-α-DA-1,3-β-G4S-1,4-α-DA-1,3-G4Srα/β) and heterozygous κ/ι-neocarrahexaose (α-DA/DA2S-1,3-β-G4S-1,4-α-DA-1,3-β-G4S-1,4-α-DA-1,3-G4Srα/β). KCOs showed no cytotoxicity in RAW264.7 macrophages, and the anti-inflammatory activity was closely correlated with the degree of polymerisation and the number of sulfated groups. κ/ι-Neocarrahexaose exhibited the highest inhibition of ROS (Reactive Oxygen Species) production in LPS-induced RAW264.7 macrophages. The MPLC-ELSD system provides a platform for large-scale fabrication of purified KCOs and affords a route to these compounds that may regulate immune defense.

1. Introduction

Carrageenan oligosaccharides (COs), the degraded carbohydrates of carrageenans, are composed of an alternating backbone of β-1,3-D-galactose (G unit) and α-1,4-D-galactose (D unit). Based on the position and number of sulfate ester units (S) and the presence of 3,6-anhydrogro-bridges (A) on D units, COs are classified into 13 types denominated by Greek letter prefixes, including κ-(DA-G4S), ι-(DA2S-G4S) and λ-(D2S6S-G2S) (Necas and Bartosikova, 2013). The functional activities of COs are closely related to the degree of polymerisation (Dp), as well as the number and position of sulfate units. However, elucidating the relationship between biological activity and structure remains challenging because large-scale fabrication the purification has not been achieved.

Inflammation is regarded as a major risk factor for the pathogenesis of cancer and various other chronic diseases. Immune cells such as macrophages regulate inflammation and host defences through secretion of cytokines including NO, interleukin-1β (IL-1β), interleukin-6 (IL-6), tumor necrosis factor-α (TNF-α) and reactive oxygen species (ROS) (Kofler, Nickel, & Weis, 2005). However, excessive expression of macrophages results in tissue damage and cell death. Therefore, modulation of macrophage activation is an effective method for preventing inflammatory responses (Alvarez-Suarez et al., 2017). COs are potential pharmaceutical agents possessing multiple bioactivities including antiviral, anti-tumour, antioxidant and immunoregulatory activities (Wang et al., 2011; Yuan et al., 2005). In particular, the immunomodulation and antitumor activities of mixed κ-carrageenan oligosaccharides (KCOs) have been investigated in S180-bearing mice, and they exert their antitumor effects by promoting the immune system (Yuan, Song, Li, Li, & Dai, 2006). The immunomodulatory function of mixed KCOs has also been studied in lipopolysaccharide (LPS)-activated microglial cells, and their biological function is closely correlated with structure, especially the sulfate groups (Yao, Xu, & Wu, 2014). However, the immunomodulatory functions of KCOs with varying Dp are

* Corresponding author at: College of Food Science, Fujian Agriculture and Forestry University, Fuzhou, 350002, China.
E-mail address: zbdfst@yeah.net (B. Zheng).

http://dx.doi.org/10.1016/j.carbpol.2017.10.043
Received 14 August 2017; Received in revised form 15 September 2017; Accepted 11 October 2017
Available online 13 October 2017
0144-8617/

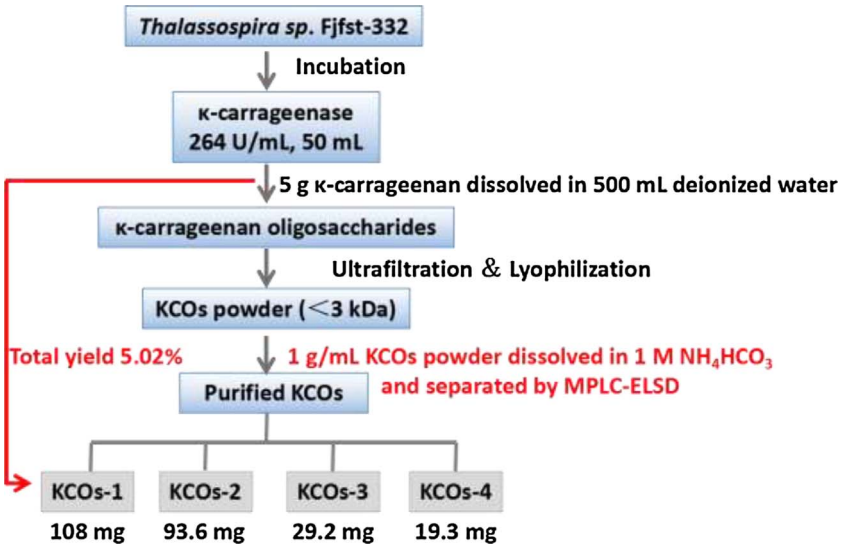

Fig. 1. Schematic diagram of KCOs enzymatic hydrolysis preparation and purification.

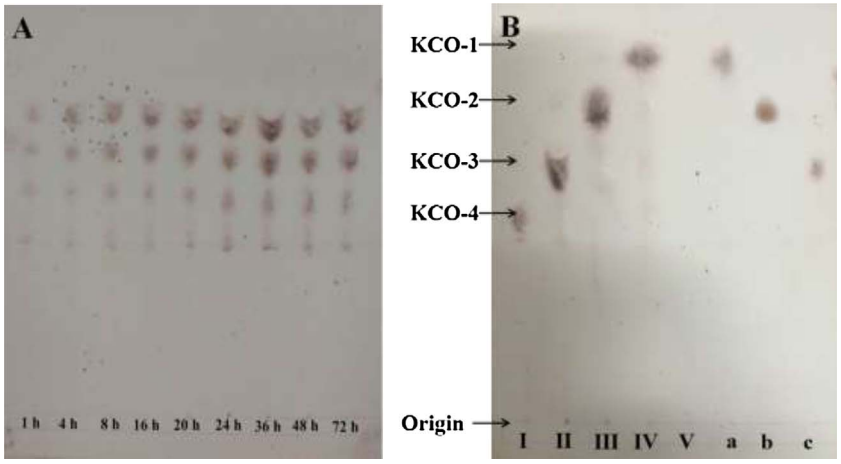

Fig. 2. TLC analysis of KCOs. (A) The components prepared through diverse enzymatic time. (B) I-V represented the components that separated by MPLC-ELSD system, a was the standards of κ-carrabiose alditols, b is the standards of κ-carratetraose alditols, c is the standards of κ-carrahexaose alditols.

not well understood, due to low yield and difficulties with purification. Thus, establishing a platform for the large-scale fabrication and purification of COs is necessary.

Column chromatographic systems consisting of a pump, detector and chromatographic column are commonly used for the separation and purification of natural products. Recently, high-pressure anion-exchange chromatography (HPAEC) (Jouanneau, Boulenguer, Mazoyer, & Helbert, 2010b), high-performance liquid chromatography-evaporative light scattering detector (HPLC-ELSD) (Niu, Zhang, Chen, & Yan, 2015), AKTA-fast protein liquid chromatography (FPLC) (Zhang et al., 2010) and high-performance gel permeation chromatography (HPGPC) (Duan, Yu, Liu, Tian, & Mou, 2016) have been used to purify COs. However, these technologies have drawbacks including a low loading amount, and can be complex to operate. Therefore, medium-pressure liquid chromatography (MPLC), a type of flash chromatography, has been developed to separate carbohydrates. This high-resolution method can be easily automated with an autosampler for peak collection (Weber, Hamburger, Schafroth, & Potterat, 2011). Furthermore, compared with the aforementioned technologies, the loading amount can be relatively high, ranging from milligrams to hectograms, facilitating large-scale separation of naturally occurring compounds (Challal et al., 2015). However, since carbohydrates do not adsorb ultraviolet (UV) light, a phenol-sulfuric acid approach is usually used for assessment, while evaporative light scattering detection (ELSD) provides an ideal detection system for carbohydrates (Young and Scientific, 2003). MPLC systems coupled with ELSD have been used for separating lotus seed oligosaccharides but not COs (Lu et al., 2017), which have a high polarity due to the sulfate groups, and varying Dp, making the preparation CO monomers challenging. Gel filtration has been used to purify COs using a Bio-Gel P-2 column (Sun et al., 2014), a Superdex 30 pg column (Niu et al., 2015), a TSK gel GMPWxl column (Zhang et al., 2010) and a Q-Sepharose Fast Flow column (Yang et al., 2011). Compared with other columns, the Superdex 30 pg column provides advantages such as high resolution, a rigid matrix, and good retention properties (Caram-Lelham, Sundelöf, & Andersson, 1995). However, when a Superdex 30 pg column is applied in HPLC or HPGPC, the low loading amount remains a limiting factor preventing large-scale purification and fabrication.

In the present study, we used MPLC coupled with ELSD and a HiLoad Superdex 30 prep grade column to separate KCOs from the Thalassospira sp. Fjfst-332 strain (Fig. 1). Compared with traditional methods, the approach removed the need for a pre-treatment operation such as desalting and depigmentation, which simplified the processing steps. Furthermore, the method provides an ideal automated, high-resolution, rapid separation compatible with a high loading amount. ESI-MS (Electrospray Ionization Mass Spectrometry), CID-MS/MS (Collision Induced Dissociation-Tandem Mass Spectrometry) and NMR (Nuclear Magnetic Resonance) were used to characterise the structural sequence,

and structure-function relationships between KCO monomers and anti-inflammatory activity were preliminarily established. The effective fabrication of KCOs will lay the foundation for studying their structure-function relationships in more detail.

2. Materials and methods

2.1. Bacteria

The κ-carrageenan-hydrolysing bacterial strain Thalassospira sp. Fjfst-332 was previously isolated from dried fragments of the red seaweed Chondrus ocellatus (collection at the Fujian Agriculture and Forestry University, China) (Guo et al., 2016).

2.2. Enzymatic preparation of KCOs

Crude κ-carrageenases (pH = 7.34 ± 0.05) (Guo et al., 2016) were added to 0.5% (w/v) κ-carrageenan solution for preparation of KCOs and incubated at 45 °C for 1 h, 4 h, 8 h, 12 h, 24 h, 30 h, 36 h, 48 h, and 72 h. Reactions were stopped by boiling at 100 °C for 5 min, then cooled to room temperature. Products were centrifuged (10,528 × g, 10 min) to remove undigested fragments, and the supernatant was

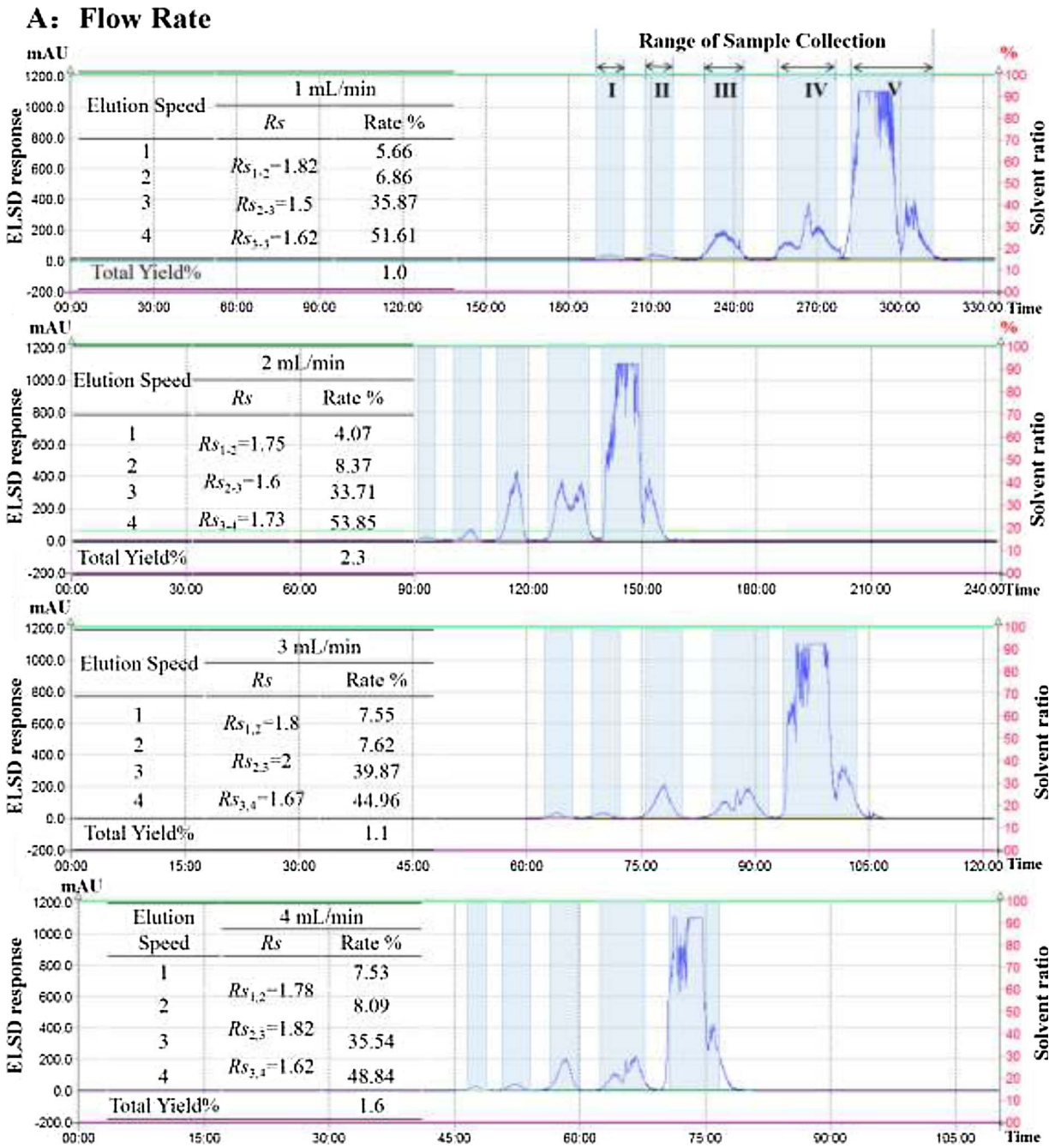

Fig. 3. The chromatogram of κ-carrageenan oligosacchrides with (A) various flow rates (sample concentration is 0.6 g/mL, the loading amount is 1 mL, the mobile phase is 0.1 M NH_4HCO_3); (B) various sample concentrations (flow rates is 4 mL/min, the loading amount is 1.0 mL, the mobile phase is 0.1 M NH_4HCO_3); (C) various loading amounts (flow rates is 4 mL/min, the sample concentration is 1.0 g/ mL, the mobile phase is 0.1 M NH_4HCO_3). The recovery rate of different components were calculated with dry powders, Rate% = [component weight (g)/total weight (g)] × 100%. The total yield was calculated with the formula of Yield % = [Total weight of oligosaccharides (g)/Substrate of κ-carrageenan (g)] × 100%. The component V was salty ions, which was analyzed with TLC (Fig. 2B).

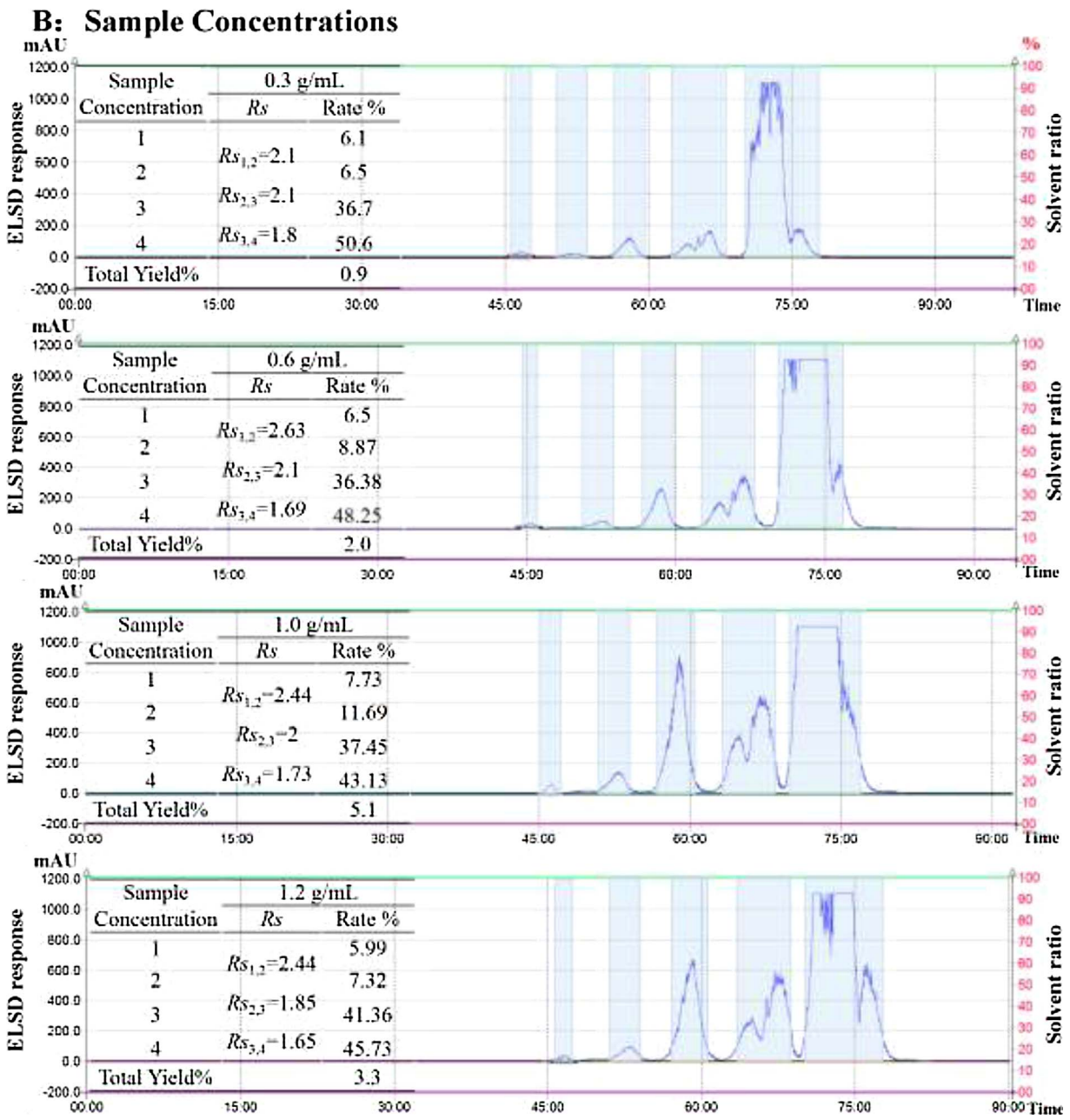

Fig. 3. (*continued*)

collected and filtered by tangential flow ultrafiltration using 10 kDa and 3 kDa membranes (Pellicon XL, Millipore Inc., Massachusetts, USA). Low molecular weight components (< 3 kDa) were collected. Fractions containing oligosaccharides were centrifuged and lyophilised for further analysis.

2.3. Separation and purification of KCOs

KCOs were separated and purified by MPLC using a modified method from that described previously (Lu et al., 2017). Data collection and system operation were controlled using Interchim Software version 5.0 (Interchim Inc., Kennedy, France). A medium pressure HiLoad™ Superdex™ 30 prep grade (26 × 600 mm, max pressure: 5 bar, max loading amount: 13 mL, adaptive flow rate: ~0.9 − 4.4 mL/min) was used for preparation with 0.1 M NH_4HCO_3 as eluent. Parameters for Flash ELSD were as follows: purging nitrogen pressure: 3.4 bar, drift tube temperature: 100 °C. KCO powders were dissolved in 0.1 M NH_4HCO_3 and filtered through a 0.22-μm microporous membrane. The column was equilibrated with 0.1 M NH_4HCO_3, and samples were injected for purification. The effects of flow rate (1 mL/min, 2 mL/min, 3 mL/min and 4 mL/min), loading amount (0.5 mL, 1 mL, 2 mL and 3 mL) and sample concentration (0.3 g/mL, 0.6 g/mL, 1 g/mL and 1.2 g/mL) on the separation were investigated and optimal parameters determined.

2.4. Resolution factor evaluation

The resolution factor (Rs) is an indicator of the separation efficiency of chromatography (Urio and Masini, 2015) calculated using the following formula:

$$Rs = \frac{V_2 - V_1}{(W_1 + W_2)/2}.$$

where V is the appearance time of the peak, and W is the retention time of the peak.

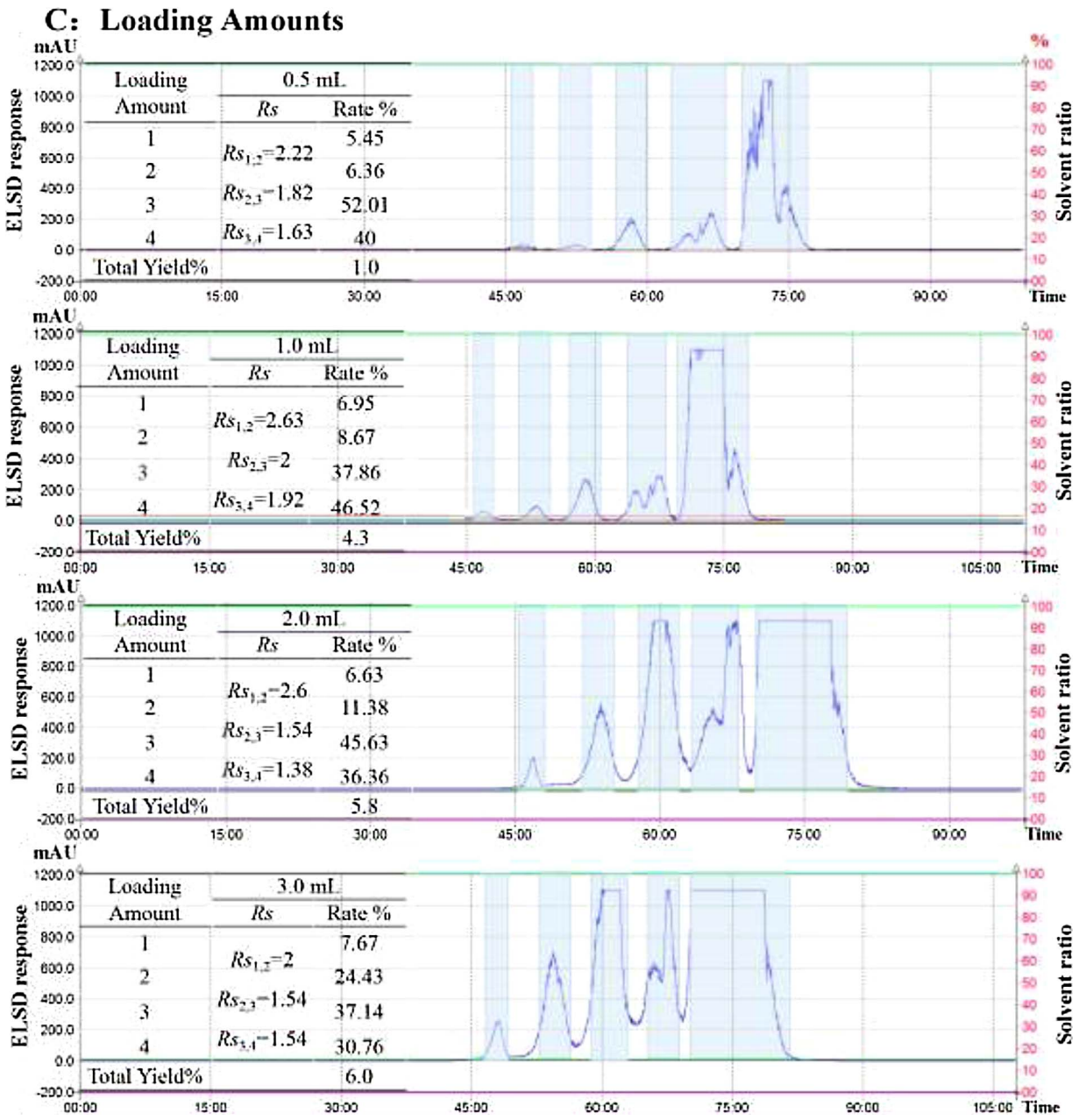

Fig. 3. (*continued*)

2.5. TLC analysis of KCOs

The KCOs were analyzed by the TLC (Thin Layer Chromatography). The lyophilized samples were redissolved in deionized water (1 mg/mL) and loaded on a 10 cm × 20 cm TLC plate. The plate was developed with a solvent mixture containing n-butane:ethanol:water (3:2:2, v/v/v). The plate was stained by spraying a mixture of vitriol:ethanol (3:17, v/v; with 0.2% resorcinol, w/v) and heating at 150 °C for 5 min until the presence of visible bands.

2.6. ESI-MS and CID MS/MS analysis

Mass spectra of KCOs were analysed using a MS system (Agilent 7890A + 5975 B MS, California, USA) equipped with an electrospray ionisation source. Data acquisition and processing were performed using MassHunter Workstation software version B.04.00 (Agilent Technologies Inc., California, USA). Analytes (1.0 mg/mL) were injected into the mass spectrometer via a 5 μL loop. ESI-MS parameters were as follows: Drying gas: N_2, flow rate: 5 L/min, temperature: 300 °C, nebulizer pressure: 45 psi, electrospray capillary voltage: 3500 V, temperature and flow rate of sheath gas: 300 °C and 11L/min, respectively. Negative ionisation mode was used and the mass scan range was ~50 − 2500 amu. CID MS/MS was carried out with helium (He) as the collision gas, and the collision energy was set at 70 V.

2.7. NMR analysis

All NMR data were recorded on a Bruker Avance III HD 400 MHz NMR spectrometer (Bruker Company, Fällanden, Switzerland) at 25 °C. Purified samples were exchanged twice in D_2O (99.7%) and redissolved in D_2O at 10 mg/mL. ^{1}H-NMR spectra of KCOs were recorded using a sweep width of 8223 Hz and 16 scans (Fidres of 0.125 Hz). ^{13}C-NMR spectra were recorded at 100 MHz with a sweep width of 24038 Hz and 1024 scans (Fidres of 0.367 Hz). ^{1}H-^{1}H COSY spectra were obtained with a sweep width of 1014 Hz in both dimensions for KCO-1 (Fidres of 0.495 Hz), 925 Hz for KCO-2 (Fidres of 0.452 Hz), 927 Hz for KCO-3

(Fidres of 0.452 Hz), and 2645 Hz for KCO-4 (Fidres of 1.292 Hz). ^{1}H-^{13}C HMQC experiments were recorded with a sweep width of 1114 Hz in both dimensions for KCO-1 (Fidres of 1.088 Hz), 793 Hz for KCO-2 (Fidres of 0.775 Hz), 2645 Hz for KCO-3 (Fidres of 2.583 Hz), and 2906 Hz for KCO-4 (Fidres of 2.906 Hz). ^{1}H-^{13}C HMBC spectra of KCO-1 were recorded with a sweep width of 1014 Hz (Fidres of 0.495 Hz), 926 Hz for KCO-2 and KCO-3 (Fidres of 0.280 Hz), and 2645 Hz for KCO-4 (Fidres of 0.646 Hz).

2.8. Cell culture and treatment

The murine RAW264.7 macrophage cell line was purchased from American Type Culture Collection (ATCC, Rockville, MD, USA). RAW264.7 cells were cultured in 90% dulbecco's modified eagle medium (DMEM) (12800-082 GIBCO, Carlsbad, California, USA) supplemented with 10% fetal calf serum (FBS) (FSS500, ExCell Biology, Carlsbad, California, USA), 100 U/mL of penicillin, 100 mg/mL of

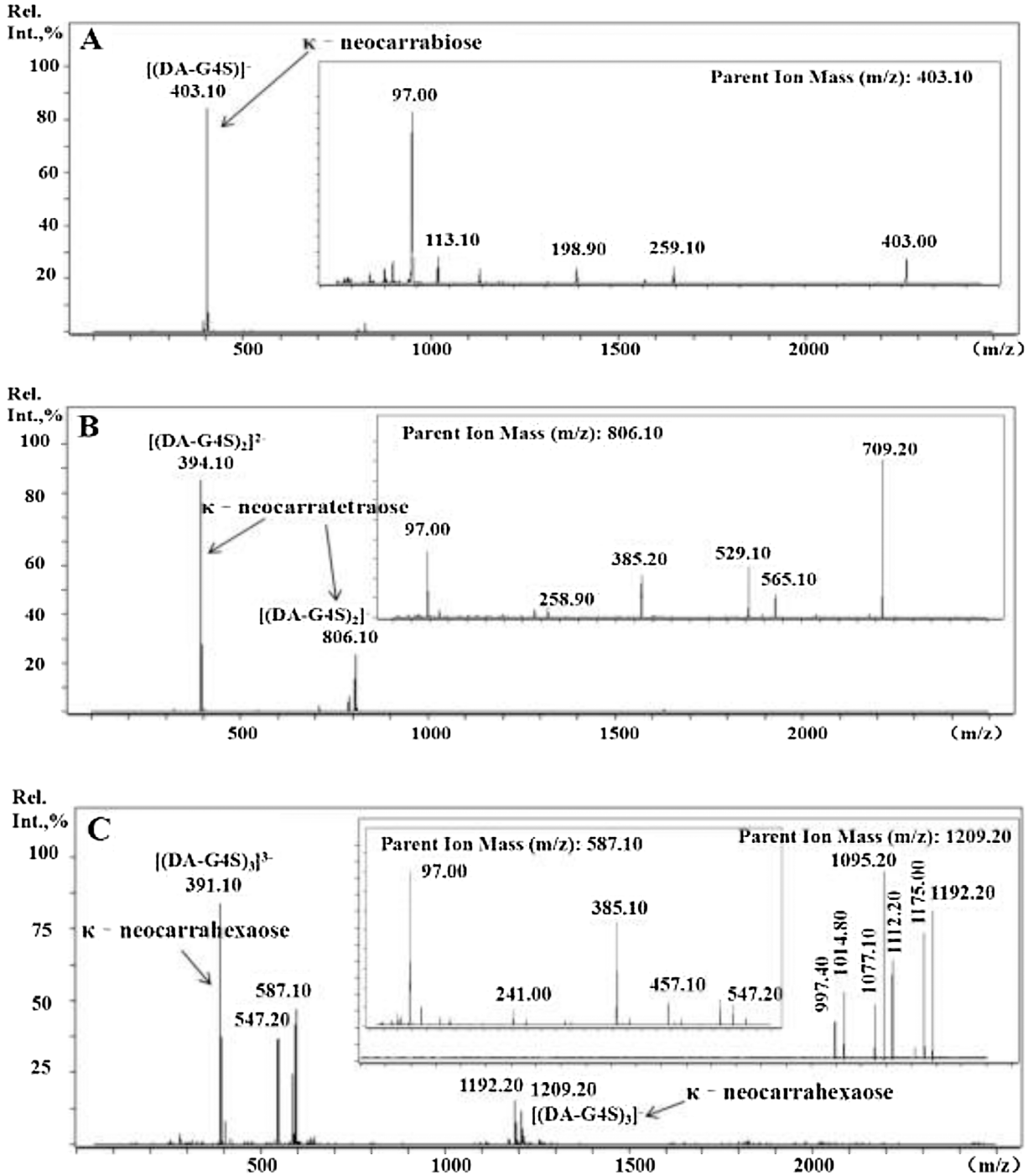

Fig. 4. (A–D) ESI-MS and CID MS/MS spectrometry analysis of KCOs that were separated through MPLC-ELSD system. The fragment ions are annotated as [DA-G4S]n, where DA is 3,6-anhydrogro-α-1,4linked-D-galactose, G4S is β-1,3-D-galactose with 4-O-sulfated groups, and n is the number of subunits. (E) The scheme of structural sequence. The non-reducing terminal fragment ions are named as A-, B- or C- type ions, and reducing terminal are designed as X-, Y- or Z- type ions.

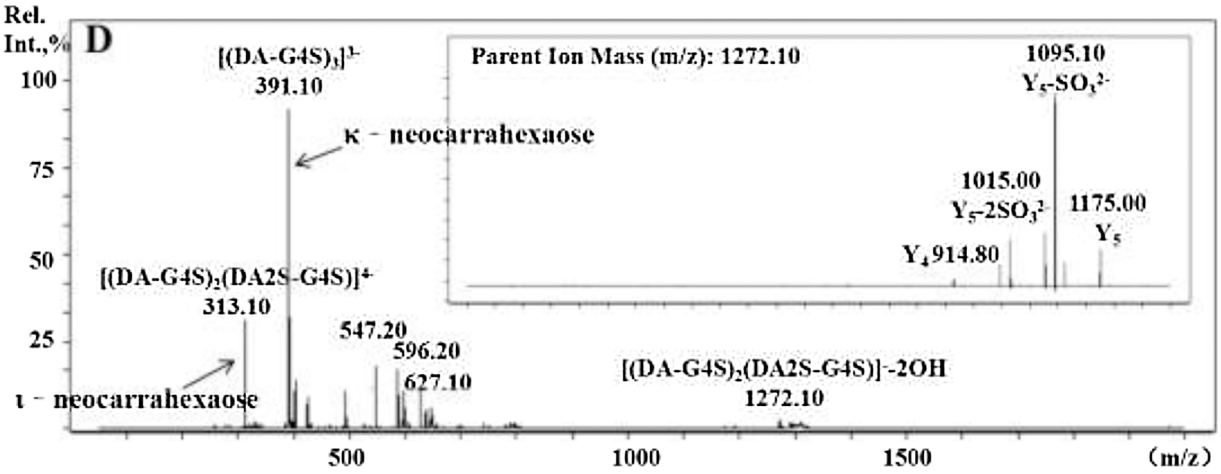

E

KCO-1 [M-H]⁻ :403 m/z DA—O—G4S

KCO-2 [M-H]⁻ :806 m/z

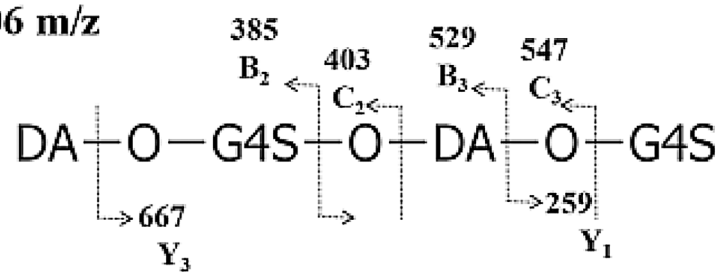

KCO-3 [M-H]⁻ :1272 m/z

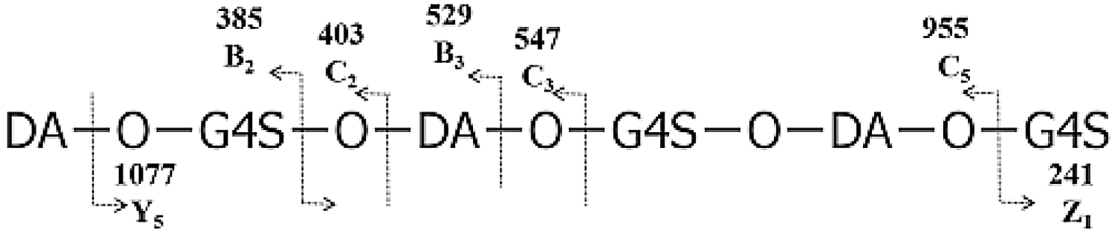

KCO-4 [M-H]⁻ :1272 m/z

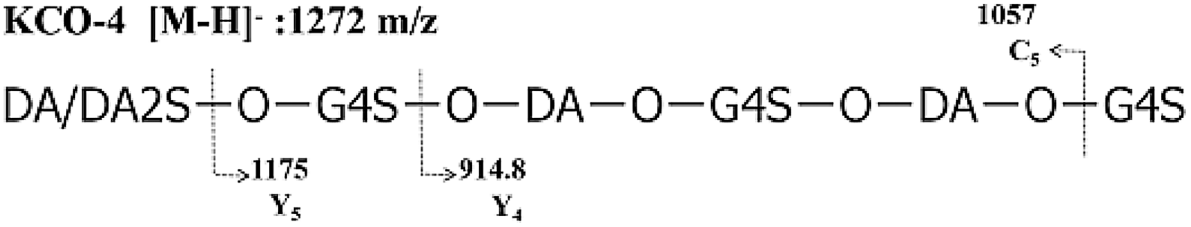

Fig. 4. (*continued*)

Table 1
^{1}H NMR data assignments for KCO-1, KCO-2, KCO-3 and KCO-4.

Residue	Chemical shift (ppm)					
	H1	H2	H3	H4	H5	H6
KCO-1						
α-DA(1→	5.06	4.07	4.33	4.45	4.39	4.02/4.13
→3)-G4Srα	5.3	3.91	3.97	4.87	3.75	3.70/3.76
→3)-G4Srβ	4.63	3.56	3.95	4.81	3.75	3.70/3.76
KCO-2						
α-DA(1→	5.06	4.11	4.38	4.46	4.39	4.02/4.18
→3)-β-G4S(1→	4.63	3.56	3.95	4.81	3.79	3.70/3.76
→4)α-DA'(1→	5.04	4.06	4.31	4.59	4.39	4.02/4.18
→3)-G4Srα	5.27	3.87	3.97	4.87	3.75	3.71/3.76
→3)-G4Srβ	4.63	3.56	3.95	4.81	3.79	3.70/3.76
KCO-3						
α-DA(1→	5.06	4.1	4.31	4.44	4.37	4.02/4.21
→3)-β-G4S(1→	4.63	3.56	3.95	4.82	3.77	3.70/3.77
→4)α-DA'(1→	5.04	4.06	4.31	4.59	4.61	4.02/4.18
→3)-G4Srα	5.28	3.87	4.12	4.85	3.75	3.71/3.76
→3)-G4Srβ	4.63	3.56	3.95	4.82	3.77	3.70/3.77
KCO-4						
α-DA(1→	5.04	4.07	4.3	4.44	4.37	4.01/4.18
α-DA2S(1→	5.25	4.65	4.82	4.64	4.61	4.01/4.18
→3)-β-G4S(1→	4.61	3.6	3.99	4.82	3.78	3.74/3.78
→4)α-DA'(1→	5.07	4.11	4.64	4.56	4.63	4.01/4.18
→3)-G4Srα	5.28	3.86	4.11	4.87	3.78	3.74/3.78
→3)-G4Srβ	4.61	3.55	3.98	4.82	3.78	3.74/3.78

*DA is 3,6-anhydrogro-α-1,4linked-D-galactose; DA' is internal 3,6-anhydrogro-α-D-galactose; G4S is β-1,3-D-galactose-4-sulfate; DA2S is 3,6-anhydrogro-α-1,4linked-D-galactose-2-sulfate.

streptomycin, and maintained in an XD-101 incubator (SANYO, Yamaguchi Prefecture, Japan) with 5% CO_2 at 37 °C. Cells were pre-incubated with purified KCOs (resuspended in DMEM to 10 μg/mL, 25 μg/mL and 50 μg/mL) and DXM (50 μg/mL, positive group) for 4 h, exposed to 10 μg/mL LPS for 24 h, or treated with DMEM only (control group) or LPS only (negative control) for 24 h.

2.9. Cell viability assay

RAW264.7 cells were seeded in 96-well plates at a density of 2×10^5 cells/mL and cultured overnight, then treated with KCO-1, KCO-2, KCO-3 or KCO-4 for 24 h. Next, 20 μL of MTT (5 mg/mL in PBS, 0793 Amresco, California, USA) was added to each well and incubated for another 4 h. The medium was removed carefully and 150 μL of DMSO (Shanghai Yijiu Company, China) was added. Plates were shaken for 10 min, and the optical density at 490 nm was measured with an ELISA microplate reader (BioTek, ELx800, Norcross, Georgia, USA). Cell viability was determined relative to untreated cells in the control group.

2.10. Measurement of intracellular ROS

Intracellular ROS levels were measured using 2′-7′-dichlorofluorescin diacetate (DCFH-DA) as previously reported (Eruslanov & Kusmartsev, 2010). After treatment, cells were washed with PBS, centrifuged (421 × g, 5 min), resuspended at a density of 1×10^6 cells/mL, and incubated with 10 μM DCFH-DA (Sigma Aldrich, St. Louis, MO, USA) at 37 °C for 20 min in the dark. After washing with PBS three times to remove free DCFH-DA, the fluorescence intensity was captured using a FACS Calibur flow cytometer (Becton-Dickinson, Franklin Lakes, New Jersey, USA) at an excitation wavelength of 488 nm and an emission wavelength of 530 nm.

2.11. Statistical analysis

All experiments were performed in triplicate. Data were analysed using the DPS statistical analysis system software (V9.50, Ruifeng Information Company, Hangzhou, China) and Origin Pro (V8.5, OriginLab, Wellesley Hills, Washington, USA). Data are presented as means ± standard deviation (SD).

3. Results and discussion

3.1. Optimisation of parameters for MPLC separation of KCOs

A gel filtration column (HiLoad™ Superdex™ 30 prep grade) that is capable of high resolution separation of the oligosaccharides and peptides with molecular weight up to 10 kDa, was used in this study (Knutsen et al., 2001). Its performance was evaluated using resolution factor (Rs) (Ó'Fágáin et al., 2011). Before separation, the products of various digested time were observed and monitored on TLC plates (Fig. 2A). The components of various digested time were consistent, and the oligosaccharides rang from disaccharide to hexasaccharide. Therefore, the crude KCOs were prepared through 48 h degradation in the next work.

3.1.1. Effect of flow rate on separation efficiency

The flow rate of mobile phase will affect the resolution and efficiency. The effects of flow rate on the separation of κ-carrageenan oligosaccharides were determined by comparing the chromatographic performance at the flow rate ranging from 1–4 ml/min. A faster flow rate significantly decreased the retention time of KCOs, but did not decrease the chromatographic resolution of KCO peaks (Fig. 3A). When the flow rate was 1 mL/min, the separation time was 5.5 h, and resulting in overlap of peak IV. At a flow rate of 4 mL/min, the separation time of KCOs was significantly shortened to less than 1.5 h. Compared with the study that reported a elution time of 3 − 6 h (Knutsen et al., 2001), the MPLC system performed faster separation time. On the other hand, the Rs value ($Rs_{1,2}$ = 1.78, $Rs_{2,3}$ = 1.82, $Rs_{3,4}$ = 1.62) and total yield of KCOs (1.6%) at 4 mL/min were relatively higher, synthetically, 4 mL/min was the better flow rate for KCO separation.

3.1.2. Effect of sample concentration and loading amount on separation efficiency

When the sample concentration was 1 g/mL, the cusp of peak III was pointed and narrow, the Rs value ($Rs_{1,2}$ = 2.44, $Rs_{2,3}$ = 2, $Rs_{3,4}$ = 1.73) were higher than under other conditions, that indicating better resolution (Fig. 3B). Furthermore, the total yield of KCOs (5.1%) was the highest. Regarding loading amount, overloading can result in severe superimposition and wider peaks, resulting in a lower yield. When the loading amount was 1 mL, the Rs value was the best as $Rs_{1,2}$ = 2.63 $Rs_{2,3}$ = 2 and $Rs_{3,4}$ = 1.92 (Fig. 3C). Even through the total yield of KCOs increased with the loading amount increased, the resolution (Rs value) decreased significantly and the peak III was flattened. Therefore, the loading amount of 1 mL is the most suitable parameter. In summary, the optimal parameters for MPLC separation of KCOs were a loading amount of 1 mL, a sample concentration of 1 g/mL, and a flow rate of 4 mL/min.

3.2. ESI-MS Analysis of KCOs

After separation and purification, TLC was performed as a preliminarily analysis of the molecular weight distribution of the five

components (Fig. 2B). Component V did not stain, indicating that it was not a carbohydrate, and possibly corresponded to ions NaCl, $NaNO_3$, $MgSO_4{\cdot}7H_2O$, K_2HPO_4, or $CaCl_2$ that were added to produce κ-carrageenase in the fermentation medium (Guo et al., 2016). The other four components were stained successfully, were of relatively high purity, and were designated KCO-1, KCO-2, KCO-3 and KCO-4, based on their structural sequences.

Thorough separation and detailed structural investigation of oligomonosaccharides are required before detailed structure and functional relationship studies. MS analysis of KCOs was conducted at negative ESI mode due to the presence of sulfate anion groups (Ekeberg, Knutsen, & Sletmoen, 2001). In the mass spectrum of KCO-1 (Fig. 4A), a solitary peak at m/z 403.1 was detected, which was assigned to κ-carrabiose $[(DA\text{-}G4S)]^-$, which has one sulfate group. The absence of other signals indicated high purity. The MS image of KCO-2 (Fig. 4B) revealed peaks at m/z 394.1 and m/z 806.2, corresponding to molecular anions $[(DA\text{-}G4S)_2]^{2-}$ and $[(DA\text{-}G4S)_2]^-$ that were assigned to κ-carratetraose with two sulfate units, and the doubly-charged $[(DA\text{-}G4S)_2]^{2-}$ anion. Peaks at m/z 391.1 and m/z 1209.1 were representative of κ-carrahexaose $[(DA\text{-}G4S)_3]^{3-}$ and $[(DA\text{-}G4S)_3]^-$ carrying three sulfate groups (Fig. 4C). The peak at m/z 547.2 corresponds to desulfated doubly-charged κ-carrahexaose $[(DA\text{-}G4S)_2(DA\text{-}G)]^{2-}$. We speculated that desulfation due to the high cone voltage was responsible, rather than the presence of β-type COs (Anastyuk et al., 2011; Sun et al., 2014). Peaks at m/z 587.1 and 1192.2 were assigned to $[(DA\text{-}G4S)_3]^{2-}$ and $[(DA\text{-}G4S)_3]^-$, which have lost a single OH^- group. Fig. 4D shows the mass spectrum of component KCO-4, with peaks at m/z 313.1, 627.1 and 1272.1 corresponding to quadruple-, doubly- and singly-charged molecular anions ι-carrahexaose $[(An\text{-}G4S)_2(An2S\text{-}G4S)]^{4-}$, $[(An\text{-}G4S)_2(An2S\text{-}G4S)]^{2-}\text{-}2OH^-$ and $[(An\text{-}G4S)_2(An2S\text{-}G4S)]^-\text{-}2OH^-$, which all have four sulfate groups. Oversulfation was attributed to a common impurity of ι-carrageenan in commercial κ-carrageenan (Sun et al., 2014). The peak at m/z 391.1 $[(An\text{-}G4S)_3]^{3-}$ was also found in the mass spectrum, thus, component KCO-4 might be the heterozygous κ/ι-carrahexaose. Furthermore, there was no other mixed peak in the four MS spectra, indicating the high purity of all four components. Characteristic ions of KCOs in mass spectra are presented in supplementary material Table S1.

3.3. Analysis of CID-MS/MS spectra of KCOs

Detailed structural information on KCOs was obtained from CID

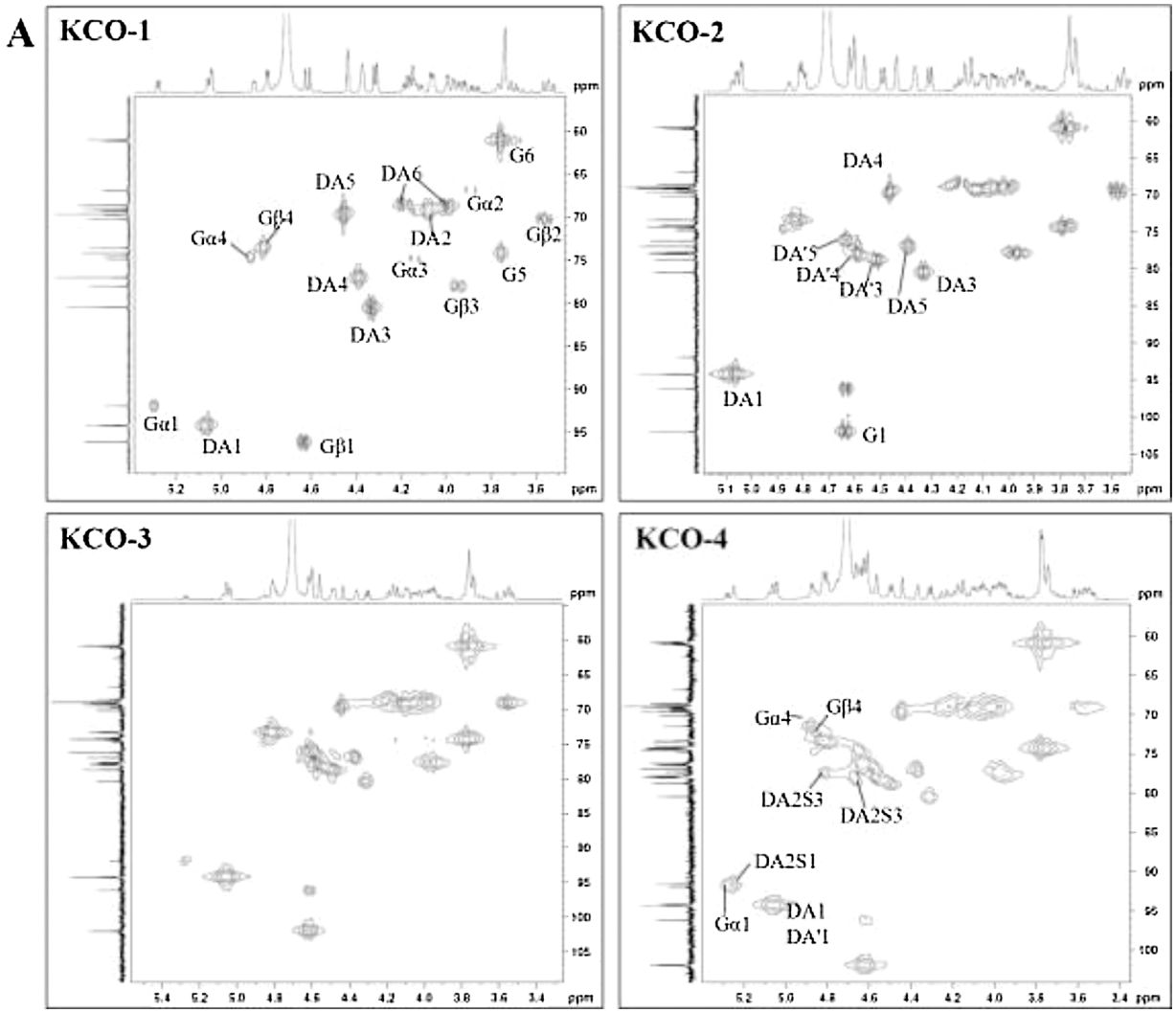

Fig. 5. (A) ^1H-^{13}C-HMQC spectra of KCO-1, KCO-2, KCO-3 and KCO-4. (B) ^1H-^1H-COSY spectra of KCO-1, KCO-2, KCO-3 and KCO-4. (C) ^1H-^{13}C-HMBC spectra of KCO-1, KCO-2, KCO-3 and KCO-4. The cross-peaks were labeled.

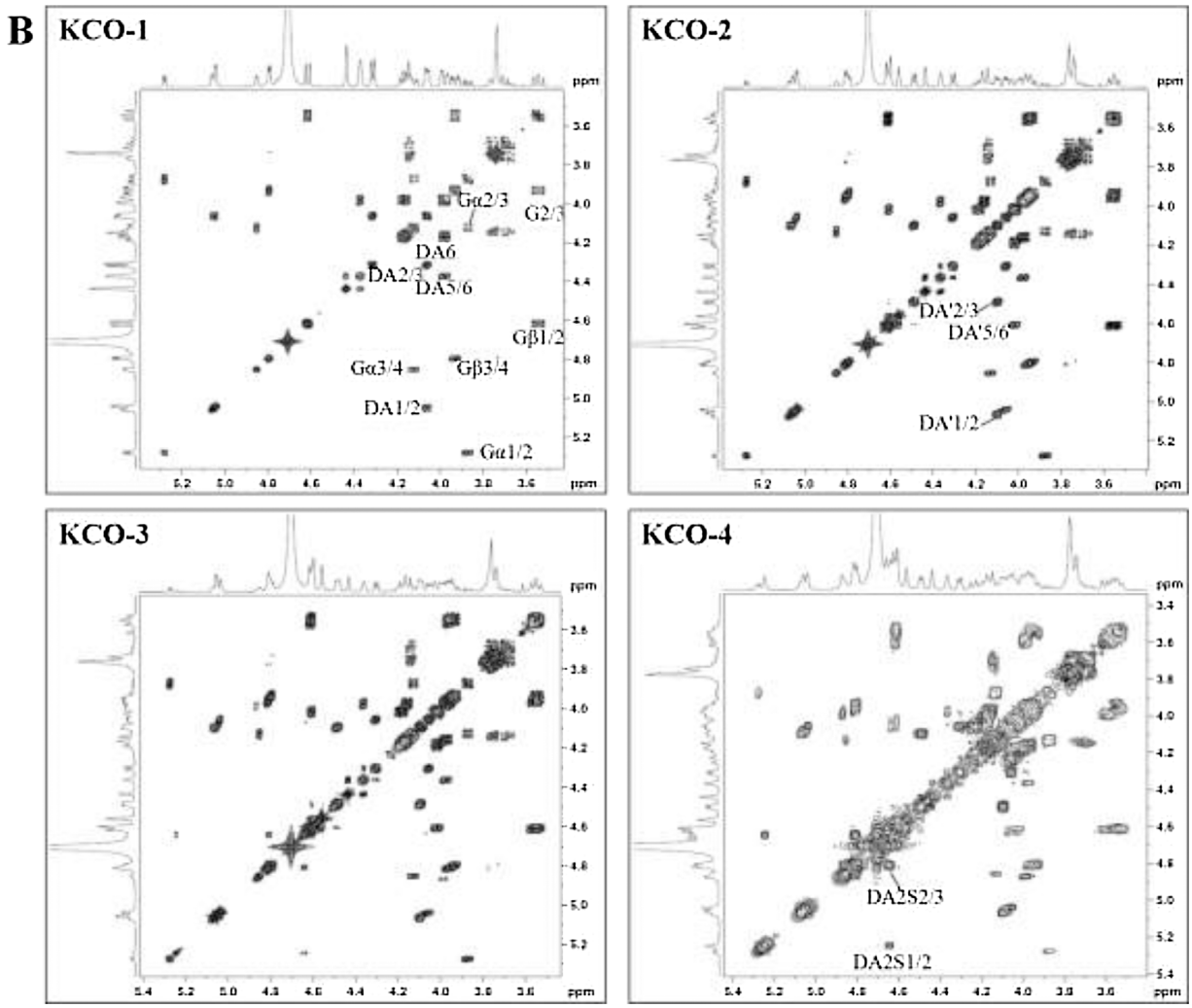

Fig. 5. (*continued*)

MS/MS. In our study, there were no precursor ions added for derivatisation, therefore, desulfation reactions occurred readily and the results were detected in the CID MS/MS spectra (Aguilan, Dayrit, Zhang, Ninonuevo, & Lebrilla, 2006). Meanwhile, the method did not reduce oligosaccharides using $NaBH_4$ to generate oligosaccharide alditols, and it was therefore not able to immediately differentiate between reducing or non-reducing fragment ions with identical masses arising from glycosidic cleavages (Sun et al., 2014; Yu et al., 2006).

In the CID MS/MS profiles of κ-carrabiose using m/z 403.1 as the parent ion, the fragment peaks m/z 113.1, 198.9 and 259.1 were relatively less abundant, since desulfation (HSO_4^-, m/z 97) would dissipate energy. The peak at m/z 113.1 was assigned to the G4S group following loss of HSO_4^- and CH_2OH^- [G4S-HSO_4^--CH_2OH^-]. The peak at m/z 198.9 was the cross-ring cleavage fragment (G4S) corresponding to $^{1,3A}_{1}$- or $^{1,3}Z_0$-type. Additionally, we did not observe other signals in the second-order spectrum, further indicating that KCO-1 was κ-carrabiose.

Compared with doubly- or triply-charged molecular ions as precursors for CID MS/MS analysis, singly-charged ions can yield more extensive structural information. MS/MS spectra of κ-carratetraose are shown in Fig. 4B based on singly-charged m/z 806.2 as parent ions. Fragment ions at m/z 97.0, 258.9, 385.2, 529.1, 565.1 and m/z 709.2 were assigned (Table S2). The G4S groups arising from non-reducing termini readily facilitate desulfation of B- and C-type ions (Yang et al., 2011). However, there were no desulfated B- or C-type fragment ions observed, indicating that oligosaccharides were assigned to κ-neocarratetraose with G4S at the reducing terminus, consistent with the structural order displayed in Fig. 4E, and indicating that KCO-1 was κ-neocarrabiose.

Based on enzyme specificity, component KCO-3 was κ-noecarrahexaose that carries G4S as the reducing terminal. When choosing singly charged ions m/z 1209.2 as parent ions, peaks at m/z 997.4, 1014.8, 997.4, 1077.1, 1095.2, 1112.2, 1175.0 and m/z 1192.2 were observed and sequences assigned (Table S2). These fragment structures were consistent with κ-noecarrahexaose losing sulfate groups or OH^-. The doubly charged ion m/z 587.1 was also chosen as a parent ion due to the lower abundance of singly-charged ions. Peaks at m/z 97.0, 241.0, 385.1, 457.1, 529.0 and m/z 547.2 were assigned (Table S2). In the obtained MS/MS profiles of κ/ι-neocarrahexaose (Fig. 4D), the glycosidic cleavage fragment ions were detected at m/z 914.8, 1015.0, 1095.1 and 1175.0, but m/z 505 signals were not detected, indicating that there were no [G4S-DA2S] fragment ions present. Thus, the component was designated as κ/ι-neocarrahexaose with DA2S groups at the non-reducing terminus, and the structural order is displayed in Fig. 4E.

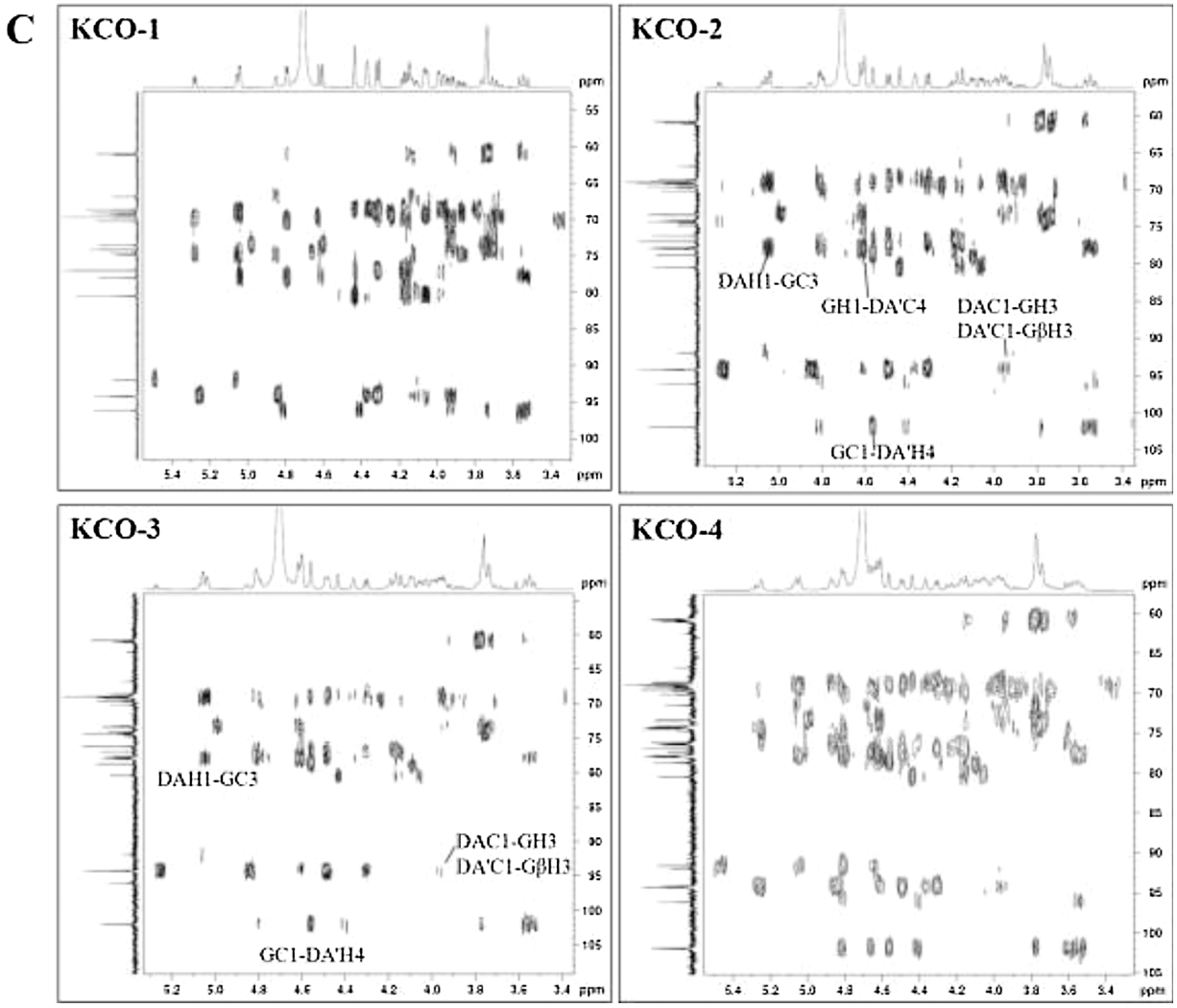

Fig. 5. (*continued*)

3.4. Analysis of the structural sequence of KCOs

The end-products of the action of TF-332-κ-carrageenase were κ-neocarrabiose, κ-neocarratetraose, κ-neocarrahexaose and κ/ι-neocarrahexaose, as confirmed by preparation and complete ^{1}H and ^{13}C NMR spectra assignment (Table 1; ^{1}H and ^{13}C NMR spectra are shown in Fig. S1). In the ^{1}H NMR spectrum of KCO-1, the peak at 5.06 ppm is the anomeric proton of 3,6-anhydrogro-α-D-galactose units, and resonant signals at 5.3 ppm (G4Sre-α-H1) and 4.63 ppm (G4Sre-β-H1) were observed. In the ^{13}C-NMR spectrum, the anomeric carbon of G4S with α and β configurations located at the reducing end were attributed to peaks at 91.98 ppm and 96.17 ppm, which were shifted in the high-field. In addition, the signal from G4S-C3 was shifted in the low-field, indicating a glycosidic linkage located at position 3, which was confirmed by ^{1}H-^{13}C HMQC (Fig. 5A). Therefore, component KCO-1 was designated as κ-neocarrabiose with a G4S unit at the reducing end, and the structural formula is α-DA-1,3-G4Srα/β. The ^{1}H-NMR spectrum of KCO-2 was similar to that of KCO-1, except the signal at 5.04 ppm, which was attributed to the α-anomeric proton of the internal 3,6-anhydrogro-α-D-galactose (α-DA'-H1). The ring proton of G4S was assigned using ^{1}H-^{1}H COSY analyses from H1 to H4 (Fig. 5B). The ^{1}H-^{13}C HMQC spectra made it possible to ascribe the correlations of H5 and H6 protons (Prechoux & Helbert, 2014). From the ^{13}C-NMR spectrum of KCO-2, the signal of the anomeric carbon at 101.96 ppm was found to correspond to 1,3-β-G4S and the sulfated group substituted at position 4. Moreover, the non-reducing end of α-DA-C1 (94.21 ppm) indicated that KCO-2 was κ-neocarratetraose with double repeating DA-G4S units (α-DA-1,3-β-G4S-1,4-α-DA-1,3-G4Srα/β). The long-rang ^{1}H-^{13}C correlations assigned in HMBC confirmed that G4S-C1 correlated with DA-H4 through the 1,4-glycosidic linkage (Fig. 5C) (Zhang et al., 2010). Based on the observation of the anomeric region of ^{1}H-^{13}C HMQC spectra, four spin systems were found and the glycosyls were assigned as pyranoses. Furthermore, the lack of a signal at 66.4 ppm (corresponding to the G4S-C4 unit without a sulfate group) suggested that desulfation did not occur during TF-332-κ-carrageenase enzymatic hydrolysis, which was also verified by ESI-MS analysis (Yuan & Song, 2005) (Table 2).

NMR spectra of KCO-3 revealed similar characteristic peaks to those of KCO-2, resulting from the close proximity of reducing and non-reducing ends. In particular, the response value of 1,4-DA and 1,3-G4S units were stronger than those observed for κ-neocarrabiose and κ-neocarratetraose. Thus, component KCO-3 was designated as κ-

Table 2
^{13}C NMR data assignments for KCO-1, KCO-2, KCO-3 and KCO-4.

Residue	Chemical shift (ppm)					
	C1	C2	C3	C4	C5	C6
KCO-1						
α-DA(1→	94.22	69.2	80.5	69.67	76.99	68.65
→3)-G4Srα	91.98	66.53	77.92	74.58	74.19	61.05
→3)-G4Srβ	96.17	70.2	77.98	73.54	74.19	61.05
KCO-2						
α-DA(1→	94.21	69.71	80.45	69.58	76.96	69.13
→3)-β-G4S(1→	101.96	69.2	78	73.39	74.36	60.84
→4)α-DA'(1→	94.27	69.71	78.76	77.9	76.96	69.2
→3)-G4Srα	91.97	66.86	77.93	74.84	74.51	61.13
→3)-G4Srβ	96.3	70.2	78	73.43	74.16	61.03
KCO-3						
α-DA(1→	94.24	69.26	80.41	69.54	76.9	68.83
→3)-β-G4S(1→	101.98	68.94	77.74	73.34	74.37	60.82
→4)α-DA'(1→	94.24	69.71	80.45	77.9	76.96	69.2
→3)-G4Srα	91.9	66.86	77.93	74.84	74.51	61.13
→3)-G4Srβ	96.3	68.94	77.74	73.34	74.37	60.82
KCO-4						
α-DA(1→	94.28	68.99	80.43	69.54	76.94	69.16
α-DA2S(1→	91.63	78.31	77.42	69.39	76.48	69.16
→3)-β-G4S(1→	101.92	68.73	77.58	73.31	74.33	60.78
→4)α-DA'(1→	94.34		79.02	77.76	76.24	69.16
→3)-G4Srα	91.97	66.86	74.5	71.73	74.33	61.03
→3)-G4Srβ	96.16	68.64	77.58	73.31	74.33	61.03

*DA is 3,6-anhydrogro-α-1,4linked-D-galactose; DA' is internal 3,6-anhydrogro-α-D-galactose; G4S is β-1,3-D-galactose-4-sulfate; DA2S is 3,6-anhydrogro-α-1,4linked-D-galactose-2-sulfate.

neocarrahexaose with the structural sequence α-DA-1,3-β-G4S-1,4-α-DA-1,3-β-G4S-1,4-α-DA-1,3-G4Srα/β. Spectra of KCO-4 were similar to those of κ-neocarrahexaose, yet the downfield signals observed at 5.25 and 91.96 ppm were attributed to sulfated DA at position 2 (α-DA2S) (Jouanneau, Boulenguer, Mazoyer, & Helbert, 2010a). Therefore, the constituent of KCO-4 was deemed to be heterozygous κ/ι-neocarrahexaose with DA and DA2S as non-reducing ends, and the structural sequence is α-DA/DA2S-1,3-β-G4S-1,4-α-DA-1,3-β-G4S-1,4-α-DA-1,3-G4Srα/β. The basic structures of κ-neocarrabiose, κ-neocarratetraose and κ-neocarrahexaose are similar to those of other KCOs produced by enzymatic hydrolysis, but different from those produced by acid hydrolysis of KCOs (Sun et al., 2015). In addition, heterozygous κ/ι-carrahexaoses are novel products from TF-332-κ-carrageenase that have not been reported previously.

3.5. Cytotoxicity of the four purified KCOs on RAW264.7 macrophages

Previous work showed that KCOs exhibit immunomodulation activity (Xu, Yao, Wu, Wang, & Zhang, 2012;Yao et al., 2014). However, most research was conducted with mixed oligosaccharides. The cell viability and potential cytotoxicity of purified κ-neo-oligosaccharides (KCO-1, KCO-2, KCO-3 and KCO-4) on RAW264.7 macrophages were evaluated (Fig. 6A). There was no evidence of cytotoxicity when the four samples were used within a concentration of 75 μg/mL in MTT assays. Cell viability was unaffected by the purified KCOs, while the inhibition rate was increased at a concentration of 300 μg/mL. These results were similar to those obtained with sulfated κ-carrageenan and human umbilical vein endothelial cells (HUVEC), in which there was no inhibition of cell growth when the concentration was lower than 100 μg/mL, and the viability was reduced to 50% when the concentration was higher than 600 μg/mL. Furthermore, substitution of sulfate groups on DA-2 may eliminate the cytotoxicity and benefit cell growth, as observed with ι-carrageenan (G4S-DA2S) (Liang, Mao, Peng, & Tang, 2014). In the present work, the heterozygous κ/ι-carrahexaoses appeared to have a synergistic effect for both G4S and DA2S, since DA2S diminished the cytotoxicity of κ-carrahexaoses, resulting in nontoxic compounds. Therefore, the degree of substitution and the position of the sulfate groups on KCOs affected cytotoxicity, and an acceptable concentration for anti-inflammatory assays was less than 75 μg/mL.

3.6. Effect of purified KCOs on ROS levels in LPS-induced RAW 264.7 macrophages

ROS are key signalling molecules in the progression of inflammatory disease, since they react and consequently damage cellular components and induce stress signalling pathways (Mittal, Siddiqui, Tran, Reddy, & Malik, 2014). The elevation of ROS production in inflammatory cells such as macrophages can cause tissue damage during inflammatory responses (Venkatesan, Park, Choi, Lee, & Kim, 2017; Zuo, Zhou, Pannell, Ziegler, & Best, 2015). In the present work, LPS increased the production of ROS in RAW 264.7 macrophages, which would damage mitochondrial membrane integrity and activate inflammatory signalling pathways. Pre-treatment with four purified KCOs significantly decreased ROS levels in cells (Fig. 6B). Furthermore, κ-neocarrahexaose displayed higher activity than κ-neocarrabiose and κ-neocarratetraose, but κ/ι-carrahexaose performed the best of the four. Inhibition of ROS production by κ/ι-carrahexaose on LPS-induced RAW 264.7 macrophages approached that of DXM (positive) controls at a concentration of 50 μg/mL. These results suggest the degree of polymerisation, as well as the number of sulfate units of κ-neocarra-oligosaccharides, affects their anti-inflammatory activity. KCOs prepared from H_2O_2 depolymerisation also suppress ROS production (Sun et al., 2015). The lower ROS levels in RAW264.7 macrophages pre-treated with KCOs might reduce the activities of MAPKs and NF-κB and enhance the mitochondrial membrane potential. Sulfated chitosan oligosaccharides reportedly inhibit LPS-induced iNOS in RAW 264.7 macrophages via JNK (Kim et al., 2014). In addition, agar oligosaccharides suppress pro-inflammatory mediator release by inducing heme oxygenase 1 (Enoki et al., 2010), and diverse sulfated marine oligosaccharides affect different signalling pathways depending on their structure. However, the signalling pathways through which KCOs affect LPS-induced RAW 264.7 macrophages remain unclear, and will be investigated in our future work.

4. Conclusions

In the present study, four types of purified κ-carrageenan oligosaccharides were separated using MPLC-ELSD, and the total yield was approximately 5.02%. The technique allows for large-scale separation, and yielded κ-neocarrabiose, κ-neocarratetraose, κ-neocarrahexaose and heterozygous κ/ι-neocarrahexaose, the structural sequences of which were confirmed using ESI-MS, CID-MS/MS and NMR analyses. Of the four, κ/ι-neocarrahexaose has highest degree of polymerisation and the largest number of sulfated groups, and exhibited the highest inhibition of ROS production in LPS-induced RAW 264.7 macrophages. Thus, the anti-inflammatory activity of κ-carrageenan oligosaccharides is significantly affected by the degree of polymerisation and the number of sulfated groups. Additional inflammatory cytokines and their effects on signalling pathways will be studied in future in vivo and in vitro work.

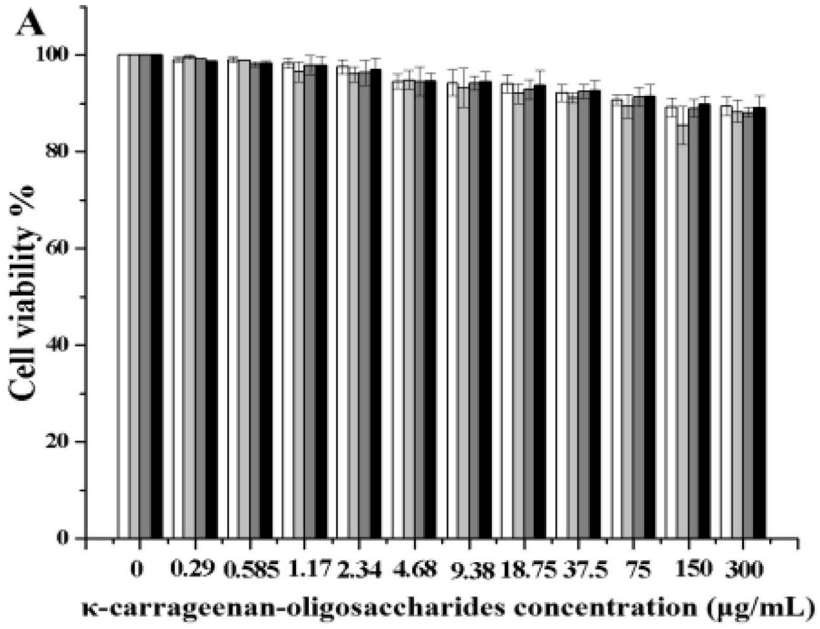

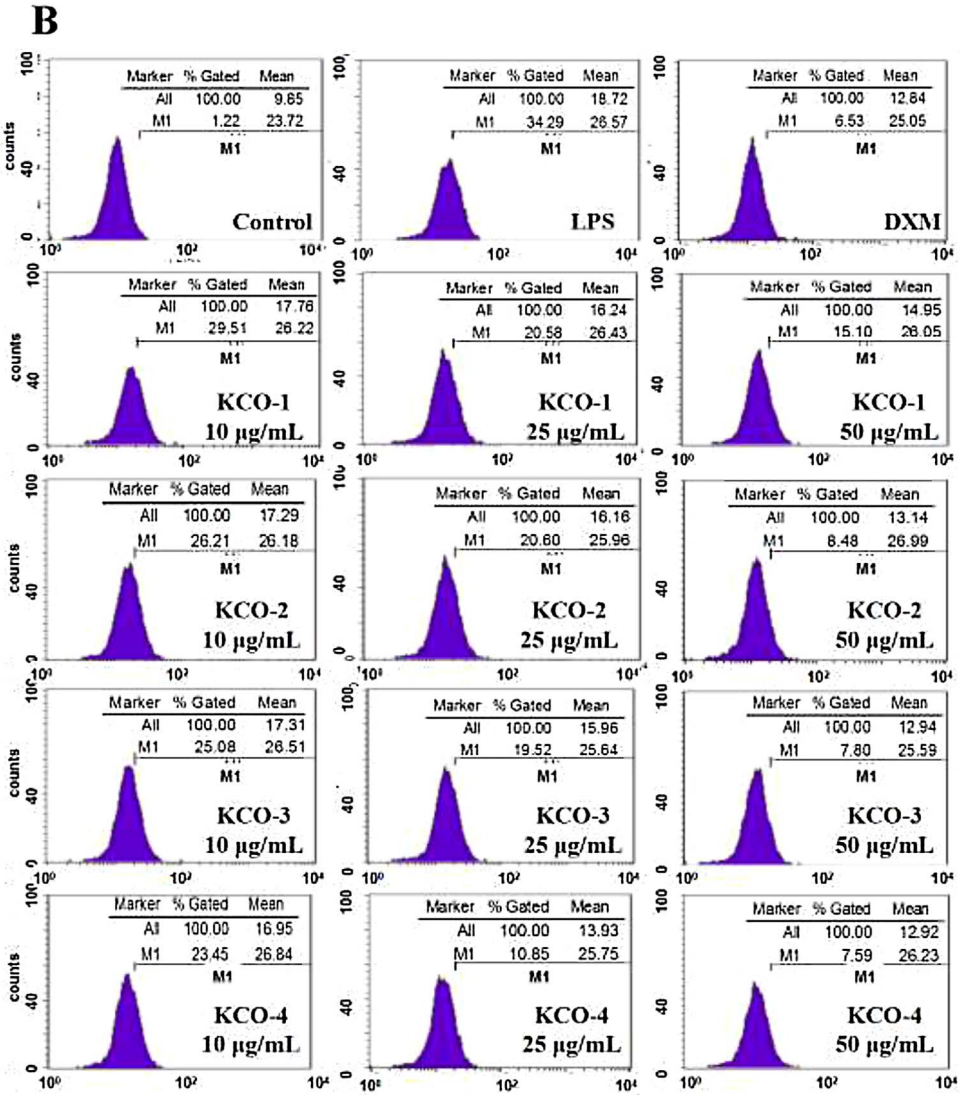

Fig. 6. (A) Cytotoxicities of four purified KCOs in RAW 264.7 macrophages determined by MTT assay. ▭ KCO-1, ▒ KCO-2, ▒ KCO-3, ■ KCO-4. (B) Effect of four KCOs on ROS production in LPS-induced RAW 264.7 cells.

Acknowledgments

We gratefully acknowledge the financial support from the National Marine Public Welfare Industry Special Scientific Research Projects (No. 201505033) and the Science and Technology Major Project of Fujian Province (No. 2015NZ0001-1).

Appendix A. Supplementary data

Supplementary data associated with this article can be found, in the online version, at http://dx.doi.org/10.1016/j.carbpol.2017.10.043.

References

Aguilan, J. T., Dayrit, F. M., Zhang, J., Ninonuevo, M. R., & Lebrilla, C. B. (2006). Structural analysis of kappa-carrageenan sulfated oligosaccharides by positive mode nano-ESI-FTICR-MS and MS/MS by SORI-CID. *Journal of the American Society for Mass Spectrom, 17*, 96–103.

Alvarez-Suarez, J. M., Carrillo-Perdomo, E., Aller, A., Giampieri, F., Gasparrini, M., Gonzalez-Perez, L., Beltran-Ayala, P., & Battino, M. (2017). Anti-inflammatory effect of Capuli cherry against LPS-induced cytotoxic damage in RAW 264.7 macrophages. *Food and Chemical Toxicology, 102*, 46–52.

Anastyuk, S. D., Barabanova, A. O., Correc, G., Nazarenko, E. L., Davydova, V. N., Helbert, W., Dmitrenok, P. S., & Yermak, I. M. (2011). Analysis of structural heterogeneity of kappa/beta-carrageenan oligosaccharides from Tichocarpus crinitus by negative-ion ESI and tandem MALDI mass spectrometry. *Carbohydrate Polymers, 86*, 546–554.

Caram-Lelham, N., Sundelöf, L. O., & Andersson, T. (1995). Preparative separation of oligosaccharides from K −carrageenan, sodium hyaluronate: and dextran by SuperdexTM 30 prep. grade. *Carbohydrate Research, 273*, 71–76.

Challal, S., Queiroz, E. F., Debrus, B., Kloeti, W., Guillarme, D., Gupta, M. P., & Wolfender, J.-L. (2015). Rational and Efficient Preparative Isolation of Natural Products by MPLC-UV-ELSD based on HPLC to MPLC Gradient Transfer. *Planta Medica, 81*, 1636–1643.

Duan, F., Yu, Y., Liu, Z., Tian, L., & Mou, H. (2016). An effective method for the preparation of carrageenan oligosaccharides directly from Eucheuma cottonii using cellulase and recombinant κ-carrageenase. *Algal Research, 15*, 93–99.

Ekeberg, D., Knutsen, S. H., & Sletmoen, M. (2001). Negative-ion electrospray ionisation-mass spectrometry (ESI-MS) as a tool for analysing structural heterogeneity in kappa-carrageenan oligosaccharides. *Carbohydrate Research, 334*, 49–59.

Enoki, T., Okuda, S., Kudo, Y., Takashima, F., Sagawa, H., & Kato, I. (2010). Oligosaccharides from agar inhibit pro-inflammatory mediator release by inducing heme oxygenase 1. *Bioscience Biotechnology Biochemistry, 74*, 766–770.

Eruslanov, E., & Kusmartsev, S. (2010). Identification of ROS using oxidized DCFDA and flow-cytometry. *Methods in Molecular Biology, 594*, 57–72.

Guo, J., Zhang, L., Lu, X., Zeng, S., Zhang, Y., Xu, H., & Zheng, B. (2016). Medium Optimization and Fermentation Kinetics for kappa-Carrageenase Production by Thalassospira sp. Fjfst -332. *Molecules,* 21.

Jouanneau, D., Boulenguer, P., Mazoyer, J., & Helbert, W. (2010a). Complete assignment of (1)H and (13)C NMR spectra of standard neo-iota-carrabiose oligosaccharides. *Carbohydrate Research, 345*, 547–551.

Jouanneau, D., Boulenguer, P., Mazoyer, J., & Helbert, W. (2010b). Enzymatic degradation of hybrid iota-/nu-carrageenan by Alteromonas fortis iota-carrageenase. *Carbohydrate Research, 345*, 934–940.

Kim, J. H., Kim, Y. S., Hwang, J. W., Han, Y. K., Lee, J. S., Kim, S. K., Jeon, Y. J., Moon, S. H., Jeon, B. T., Bahk, Y. Y., & Park, P. J. (2014). Sulfated chitosan oligosaccharides suppress LPS-induced NO production via JNK and NF-kappaB inactivation. *Molecules, 19*, 18232–18247.

Knutsen, S. H., Sletmoen, M., Kristensen, T., Barbeyron, T., Kloareg, B., & Potin, P. (2001). A rapid method for the separation and analysis of carrageenan oligosaccharides released by iota- and kappa −carrageenase. *Carbohydrate Research, 331*, 101–106.

Kofler, S., Nickel, T., & Weis, M. (2005). Role of cytokines in cardiovascular diseases: a focus on endothelial responses to inflammation. *Clinical Science, 108*, 205–213.

Liang, W., Mao, X., Peng, X., & Tang, S. (2014). Effects of sulfate group in red seaweed polysaccharides on anticoagulant activity and cytotoxicity. *Carbohydrate Polymers, 101*, 776–785.

Lu, X., Zheng, Z., Miao, S., Li, H., Guo, Z., Zhang, Y., Zheng, Y., Zheng, B., & Xiao, J. (2017). Separation of Oligosaccharides from Lotus Seeds via Medium-pressure Liquid Chromatography Coupled with ELSD and DAD. *Scientific Reports, 7*, 44174.

Mittal, M., Siddiqui, M. R., Tran, K., Reddy, S. P., & Malik, A. B. (2014). Reactive oxygen species in inflammation and tissue injury. *Antioxidants Redox Signaling, 20*, 1126–1167.

Necas, J., & Bartosikova, L. (2013). Carrageenan: a review. *Veterinami Medicina, 58*, 187–205.

Niu, T. T., Zhang, D. S., Chen, H. M., & Yan, X. J. (2015). Modulation of the binding of basic fibroblast growth factor and heparanase activity by purified lambda-carrageenan oligosaccharides. *Carbohydrate Polymers, 125*, 76–84.

Ó'Fágáin, C., Cummins, P. M., & O'Connor, B. F. (2011). Gel-Filtration Chromatography. *Methods in Molecular Biology, 36*, 1.

Prechoux, A., & Helbert, W. (2014). Preparation and detailed NMR analyses of a series of oligo-alpha-carrageenans. *Carbohydrate Polymers, 101*, 864–870.

Sun, Y., Liu, Y., Jiang, K., Wang, C., Wang, Z., & Huang, L. (2014). Electrospray ionization mass spectrometric analysis of kappa-carrageenan oligosaccharides obtained by degradation with kappa-carrageenase from Pedobacter hainanensis. *Jouranl of Agricultural and Food Chemistry, 62*, 2398–2405.

Sun, Y., Yang, B., Wu, Y., Liu, Y., Gu, X., Zhang, H., Wang, C., Cao, H., Huang, L., & Wang, Z. (2015). Structural characterization and antioxidant activities of kappa-carrageenan oligosaccharides degraded by different methods. *Food Chemistry, 178*, 311–318.

Urio, R. P., & Masini, J. C. (2015). Evaluation of Monolithic and Core-Shell Columns for Separation of Triazine Herbicides by Reversed Phase High Performance Liquid Chromatography. *Journal of the Brazilian Chemical Society, 26*, 2331–2338.

Venkatesan, T., Park, E. J., Choi, Y. W., Lee, J., & Kim, Y. K. (2017). Anti-inflammatory activity of Ternstroemia gymnanthera stem bark extracts in bacterial lipopolysaccharide-stimulated RAW264.7 murine macrophage cells. *Pharmaceutical Biology, 55*, 837–846.

Wang, W., Zhang, P., Hao, C., Zhang, X. E., Cui, Z. Q., & Guan, H. S. (2011). In vitro inhibitory effect of carrageenan oligosaccharide on influenza A H1N1 virus. *Antiviral Research, 92*, 237–246.

Weber, P., Hamburger, M., Schafroth, N., & Potterat, O. (2011). Flash chromatography on cartridges for the separation of plant extracts: rules for the selection of chromatographic conditions and comparison with medium pressure liquid chromatography. *Fitoterapia, 82*, 155–161.

Xu, L., Yao, Z., Wu, H., Wang, F., & Zhang, S. (2012). The immune regulation of kappa-carrageenan oligosaccharide and its desulfated derivatives on LPS-activated microglial cells. *Neurochemistry International, 61*, 689–696.

Yang, B., Yu, G., Zhao, X., Ren, W., Jiao, G., Fang, L., Wang, Y., Du, G., Tiller, C., Girouard, G., Barrow, C. J., Ewart, H. S., & Zhang, J. (2011). Structural characterisation and bioactivities of hybrid carrageenan-like sulphated galactan from red alga Furcellaria lumbricalis. *Food chemistry, 124*, 50–57.

Yao, Z. A., Xu, L., & Wu, H. G. (2014). Immunomodulatory function of kappa-carrageenan oligosaccharides acting on LPS-activated microglial cells. *Neurochemical Research, 39*, 333–343.

Young, C. S., & Scientific, S. (2003). Success with Evaporative Light-Scattering Detection. *LC-GC Europe, 16*, 132.

Yu, G., Zhao, X., Yang, B., Ren, S., Guan, H., Zhang, Y., Lawson, A. M., & Chai, W. (2006). Sequence determination of sulfated carrageenan-derived oligosaccharides by high-sensitivity negative-ion electrospray tandem mass spectrometry. *Analytical Chemistry, 78*, 8499–8505.

Yuan, H., & Song, J. (2005). Preparation: structural characterization and in vitro antitumor activity of kappa-carrageenan oligosaccharide fraction from Kappaphycus striatum. *Journal of Applied Phycology, 17*, 7–13.

Yuan, H., Song, J., Li, X., Li, N., & Dai, J. (2006). Immunomodulation and antitumor activity of kappa-carrageenan oligosaccharides. *Cancer Letters, 243*, 228–234.

Yuan, H., Zhang, W., Li, X., Lu, X., Li, N., Gao, X., & Song, J. (2005). Preparation and in vitro antioxidant activity of kappa-carrageenan oligosaccharides and their oversulfated, acetylated, and phosphorylated derivatives. *Carbohydrate Research, 340*, 685–692.

Zhang, W., Liu, M., Hansen, P. E., Yu, G. L., Yang, B., & Zhao, X. (2010). SEQUENCE AND STRUCTURAL ANALYSIS OF kappa-CARRAGEENAN-DERIVED OLIGOSACCHARIDES BY TWO-DIMENSIONAL NUCLEAR MAGNETIC RESONANCE1. *Journal of Phycology, 46*, 831–838.

Zuo, L., Zhou, T., Pannell, B. K., Ziegler, A. C., & Best, T. M. (2015). Biological and physiological role of reactive oxygen species–the good, the bad and the ugly. *Acta Physiologica, 214*, 329–348.